Chinese Journal of Physics 83 (2023) 287–291

Contents lists available at ScienceDirect

Chinese Journal of Physics

journal homepage: www.sciencedirect.com/journal/chinese-journal-of-physics

Weak antilocalization and localization in Cd_3As_2 thin film

Tatyana B. Nikulicheva [a,*], Vasilii S. Zakhvalinskii [a], Evgeny A. Pilyuk [a], Oleg N. Ivanov [a,b], Alexander A. Morocho [a,c], Vitaly B. Nikulichev [b], Maksim N. Yapryntsev [a]

[a] *Belgorod National Research University, Belgorod, 308015 Russia*
[b] *Belgorod State Technological University named after V.G. Shukhov, Belgorod, 308012, Russia*
[c] *Higher Polytechnic School of Chimborazo, Riobamba, 060155, Ecuador*

ARTICLE INFO

Keywords:
Weak antilocalization
Weak localization
Dirac materials
Cd_3As_2

ABSTRACT

In this work we present the results of magnetoresistance (*MR*) examination for a Cd_3As_2 thin film (with thickness of ∼ 80 nm) deposited on sapphire substrate. Within the temperature 2–10 K range, the effect of weak antilocalization (WAL) was observed. From the study of magnetoresistance, WAL appears due to surface states and is well described by Hikami-Larkin-Nagaoki model. The calculated value of the phase coherence length L_φ changes as a function of temperature T according to the power law $L_\varphi \sim T^{-0.43}$, which indicates the presence of 2D topological surface states.

1. Introduction

Dirac materials, such as graphene and topological insulators (TIs), are attracting attention due to the possibility of their use in next – generation electronic devices [1–3]. Topological insulators are a new quantum state of matter in which two-dimensional (2D) surface and one-dimensional (1D) edge states can coexist, resulting in an insulating bulk and conducting surface states [4]. Cd_3As_2 is a typical 3D Dirac semimetal material, and Weyl semimetal state can be obtained by breaking the symmetry or reducing the dimensions in Cd_3As_2 [5]. Cd_3As_2 has attracted intensive research interest since the study of the mechanism of electron transport in bulk crystals revealed the presence of new phenomena such as high mobility, giant magnetoresistance, nontrivial quantum oscillations, and splitting of Landau levels under the action of a magnetic field [6–9]. In addition, superconductivity is observed on the surface of Cd_3As_2 crystals [10], and negative magnetoresistance presented in Cd_3As_2 nanowires confirms the existence of chirality in Weyl fermions [11]. The 2D topological surface state is an important feature of 3D Dirac semimetal, which was observed on the (112) and (001) planes, respectively [12,13]. The WAL effect was also observed in Cd_3As_2 thin films [14].

In this work, we report analyze features in the magnetoresistance and weak anti-localization (WAL) originating from the amorphous Cd_3As_2 thin films.

2. Crystal structure

Cd_3As_2 thin films (∼80 nm) were obtained on a α-Al_2O_3 (001) substrate by magnetron sputtering at a pressure of 8×10^{-3} mbar.

* Corresponding author.
E-mail address: nikulicheva@bsu.edu.ru (T.B. Nikulicheva).

https://doi.org/10.1016/j.cjph.2023.03.020
Received 23 September 2022; Received in revised form 17 February 2023; Accepted 21 March 2023
Available online 22 March 2023

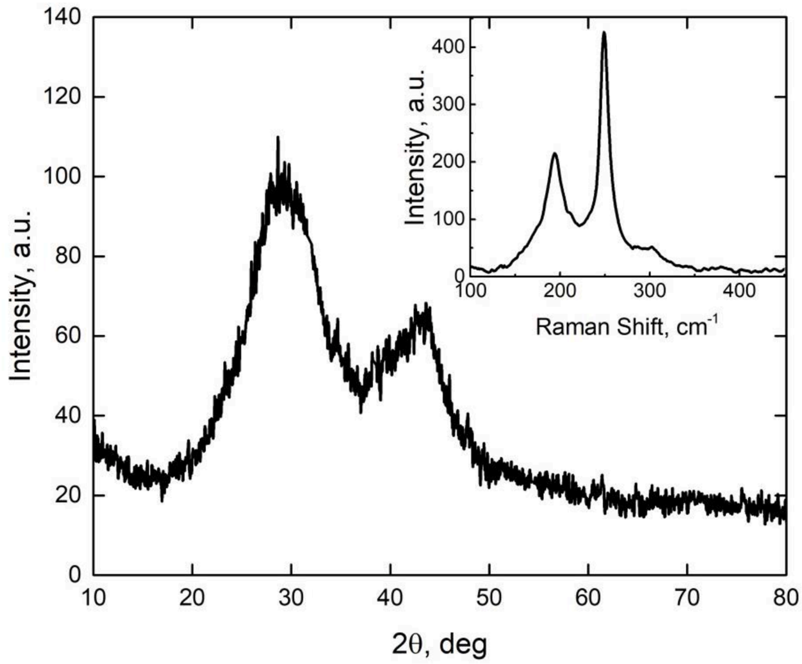

Fig. 1. Diffraction pattern of a Cd_3As_2 thin film sample deposited on sapphire substrate. The Raman spectrum is shown in inset.

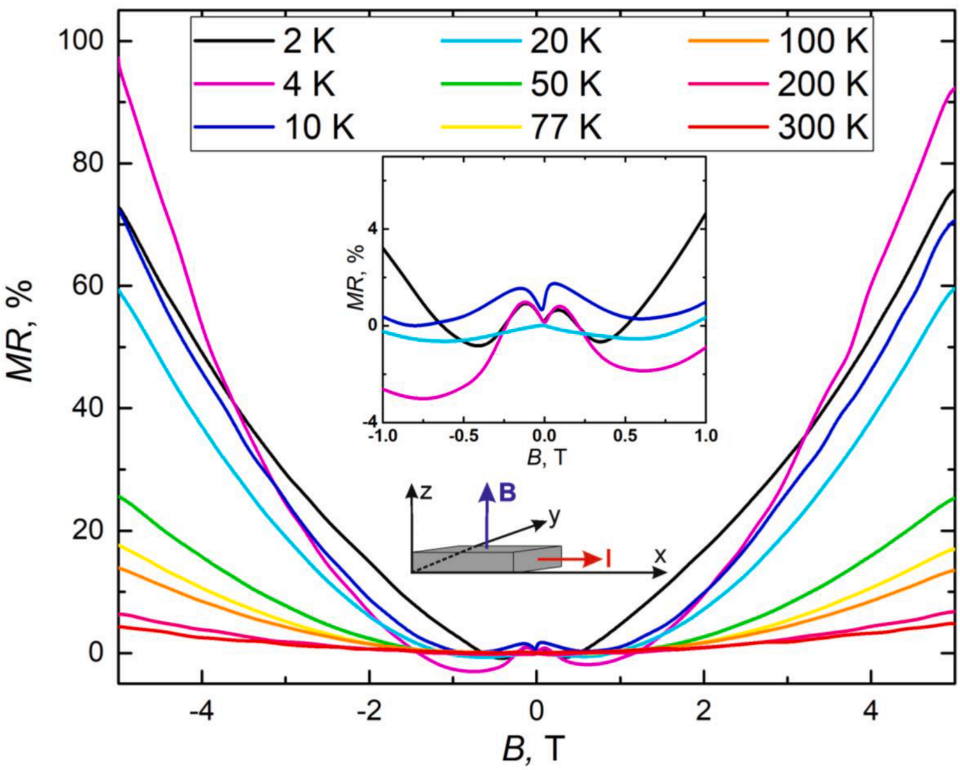

Fig. 2. Normalized magnetoresistance as a function of magnetic field B at temperatures T = 2, 4, 10, 20, 50, 77, 100, 200 and 300 K. Schematic diagram of electrical transport measurements and MR curves at 2, 4, and 10 K and low magnetic field are shown in insets respectively.

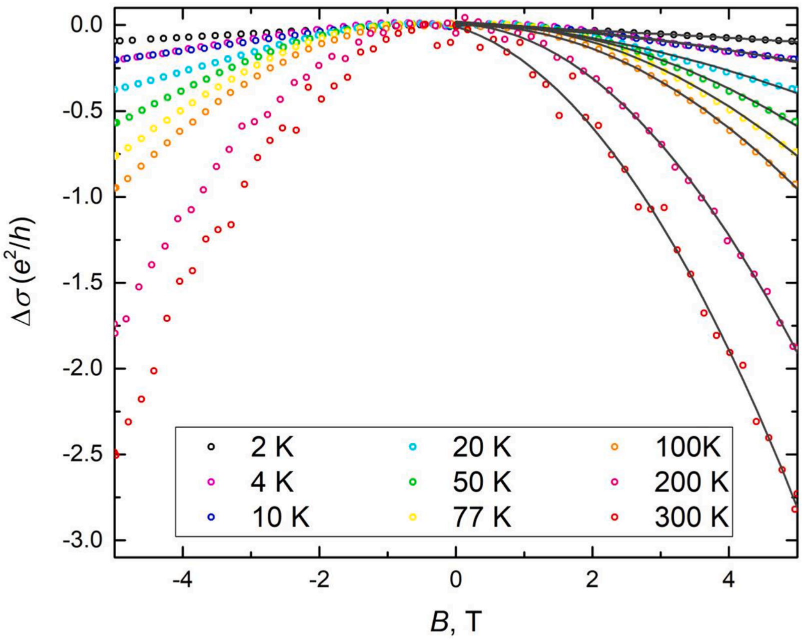

Fig. 3. Change of magnetic conductivity Δσ in the presence of an applied magnetic field with fitting (dark gray solid curves) to the Eq. (1).

The deposition rate at an applied power of 10 W and a target–substrate distance was about 1 nm/min. The substrate temperature during deposition was 20 °C. A target was used as the cathode, which was a polycrystalline disk 40 mm in diameter and 3 mm thick. The synthesis of Cd_3As_2 for the target was carried out by direct fusion of Cd and As in vacuum. The quality control of the obtained Cd_3As_2 films using X-ray methods on a Rigaku SmartLab (Rigaku corp., Japan) diffractometer and Raman spectroscopy on a LabRam HR Evolution (HORIBA JOBIN YVON S.A.S., France) was carried out. The Cd_3As_2 films were characterized by a diffraction pattern typical of amorphous materials, with broad "halo" peaks (Fig. 1).

Fig. 1 shows a X-ray scattering curve of Cd_3As_2 films. There are diffuse peaks characterized by a diffraction pattern typical of amorphous and nanocrystal materials [15,16]. The presence of the Cd_3As_2 phase in the obtained films is confirmed by Raman spectroscopy obtained using a LabRam HR Evolution, $L = 532$ nm. The spectrum shown in the inset in Fig. 1 has two pronounced peaks (at 194 and 249 cm^{-1}) characteristic of Cd_3As_2 films [17].

Magnetoresistance was measured in a standard four-probe configuration by a Mini Cryogen Free Measurements System (Cryogenic Ltd., UK).

3. Results and discussion

Fig. 2 shows the magnetic field (magnetic field B perpendicular to the electric field E) dependence of the normalized magnetoresistance (*MR*) taken at different temperatures.

Magnetoresistance is defined as $MR = [\rho(B) – \rho(0)]/\rho(0)] \times 100\%$, where $\rho(B)$ and $\rho(0)$ are the resistivities in the presence of magnetic field B and zero magnetic field, respectively. In a magnetic field of 5 T, the *MR* value changes from 4% at 300 K to 95% at 4 K. The *MR* peak observed in the low magnetic field region (Fig. 2) at $T = 2$, 4, and 10 K can be originated from weak antilocalization (WAL) effect. The presence of WAL is characteristic of Cd_3As_2 compounds due to the presence of strong spin-orbit interaction [18]. WAL effect is typical for 2D surface states bulk single crystals and thin films [14,19,20] is a signature of topological surface states.

The inset in Fig. 2 shows that the *MR* curves at 2, 4, and 10 K consist of two components: 1) negative *MR*, forming a smooth valley at ± 0.4 T for 2 K (± 0.75 T for 4 and 10 K), and 2) a *MR* positive peak at ± 0.12 T. On the other hand, only a smooth segment of *MR* appears at a higher temperature of 20 K. The positive *MR* peak corresponds to WAL due to a surface sate transition. Negative *MR* can be interpreted as the result of weak localization (WL) due to the small thickness of the film. Furthermore, the bulk state inside the film is quantized into 2D layers, thus one can expect a WL transition by passing through these quantized layers [21].

To study the WAL effect, the change in conductivity when a magnetic field is applied can be described by the Hikami - Larkin - Nagaoka (HLN) equation [14,22]:

$$\Delta\sigma(B) = \alpha\frac{e^2}{2\pi^2\hbar}\left[\ln\left(\frac{B_\phi}{B}\right) - \Psi\left(0.5+\frac{B_\phi}{B}\right)\right] + cB^2, \tag{1}$$

where $\Delta\sigma(B) = \sigma(B) - \sigma(0)$ is the magnetic conductivity, $\sigma = L/[W \cdot R(B)]$ is the electrical conductivity, L and W are the length and width of the sample, respectively, $R(B)$ is the resistance in an applied magnetic field B⊥E, $\Psi(x)$ is the digamma function,$B_\phi = \hbar/(4eL_\phi^2)$

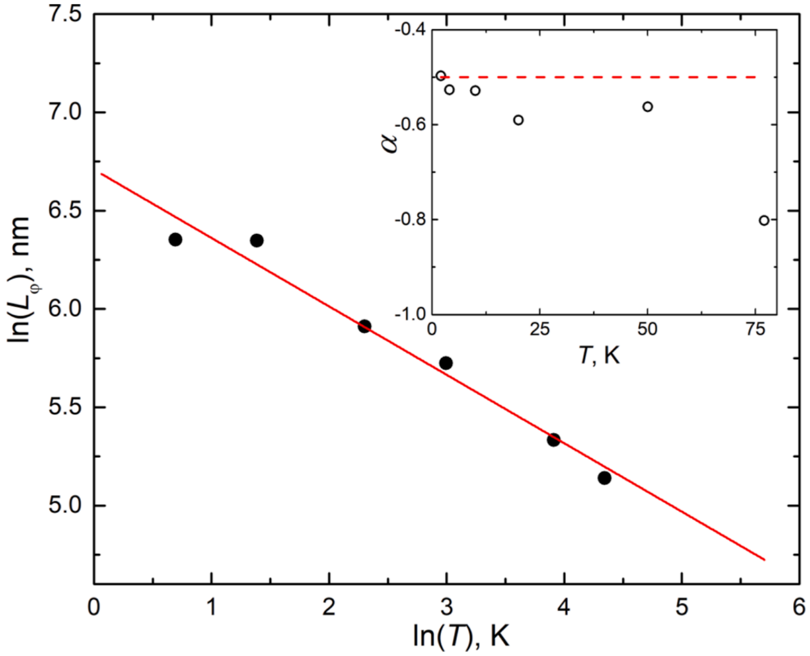

Fig. 4. Temperature dependence of ln(L_φ) (from T = 2 to 77 K). The solid red line shows the change in L_φ according to ln(L_φ) ~ –0.43·ln(T). The inset shows the temperature dependence of the prefactor α from Eq. (1) in the temperature of T = 2 – 77 K.

is the characteristic field, and L_φ is the phase coherence length.

Fig. 3 shows the change of magnetoconductivity $\Delta\sigma(B) = \sigma(B) - \sigma(0)$ in an applied magnetic field (from –5 to 5 T).

The steepness of the peaks observed at zero magnetic field in Fig. 2 at T = 2, 4, and 10 K depends on the value of the phase coherence length L_φ, which is a characteristic parameter for quantum interference effects. The L_φ value decreases from 573 nm to 119 nm with the increase of temperature from 2 K to 77 K (Fig. 4). The prefactor $\alpha \approx -0.50$ is practically independent of temperature in the range of $T = 2 - 10$ K, as shown in the inset to Fig. 4. The dimension of the 2D system is also confirmed by the temperature dependence of L_φ. Theoretically, for electron-electron scattering, the phase coherence length is proportional to temperature following the relations $L_\varphi \sim T^{-1/3}$, $L_\varphi \sim T^{-1/2}$, and $L_\varphi \sim T^{-3/4}$ for 1D, 2D and 3D systems, respectively [23]. Fig. 4 shows an approximate curve that changes according to the power-law temperature dependence $L_\varphi \sim T^{-0.43}$ (solid curve), which is very close to the expected function $T^{-0.5}$ for thin films.

At temperatures above 10 K, the α value decreases. A possible explanation for the temperature behavior of α can be interpreted as a relationship between surface and bulk states or between different surface states [24]. Thus, if there is a relationship between different conducting channels due to scattering of carriers from one conducting channel to another (preserving the phase coherence), they can contribute to the conductivity as a single phase-coherent channel.

4. Conclusion

In summary, we have measured the magnetoresistance of the Cd_3As_2 film with thickness of ~80 nm under applied magnetic field $B \perp E$. The negative MR at 2–10 K in weak magnetic field is observed. It can be interpreted as the result of WL due to the small thickness of the Cd_3As_2 film. The positive MR at the temperature higher of 20 K corresponds to WAL due to a surface sate transition. The phase coherence length changes as a function of temperature T according to the power law $L_\varphi \sim T^{-0.43}$ which is very close to the expected function $T^{-0.5}$ for thin films. It indicates the presence of 2D topological surface states.

Data availability statement

The data that supports the findings of this study are available within the article.

Declaration of Competing Interest

The authors declare that they have no known competing financial interests or personal relationships that could have appeared to influence the work reported in this paper.

References

[1] D. Kong, Y. Cui, Opportunities in chemistry and materials science for topological insulators and their nanostructures, Nat. Chem. 3 (2011), https://doi.org/10.1038/nchem.1171, 845.

[2] A.R. Mellnik, J.S. Lee, A. Richardella, J.L. Grab, P.J. Mintun, M.H. Fischer, A. Vaezi, A. Manchon, E.-A. Kim, N. Samarth, D.C. Ralph, Spin-transfer torque generated by a topological insulator, Nature 7510 (2014) 449–451, https://doi.org/10.1038/nature13534, 511.

[3] X.-L. Qi, S.-C. Zhang, Topological insulators and superconductors, Rev. Mod. Phys. 83 (2011) 1057, https://doi.org/10.1103/RevModPhys.83.1057.

[4] M.Z. Hasan, C.L. Kane, Colloquium: topological insulators, Rev. Mod. Phys. 82 (2010) 3045–3067, https://doi.org/10.1103/RevModPhys.82.3045.

[5] Z. Wang, H. Weng, Q. Wu, X. Dai, Three-dimensional Dirac semimetal and quantum transport in Cd_3As_2, Phys. Rev. B. 88 (2013), 125427, https://doi.org/10.1103/PhysRevB.88.125427.

[6] S. Jeon, B.B. Zhou, A. Gyenis, B.E. Feldman, I. Kimchi, A.C. Potter, Q.D. Gibson, R.J. Cava, A. Vishwanath, A. Yazdani, Landau quantization and quasiparticle interference in the three-dimensional Dirac semimetal Cd_3As_2, Nat. Mater. 13 (2014), https://doi.org/10.1038/nmat4023, 851.

[7] A. Narayanan, M.D. Watson, S.F. Blake, N. Bruyant, L. Drigo, Y.L. Chen, D. Prabhakaran, B. Yan, C. Felser, T. Kong, P.C. Canfield, A.I. Colea, Linear Magnetoresistance caused by mobility fluctuations in n-doped Cd_3As_2, Phys. Rev. Letts. 114 (2015), 117201, https://doi.org/10.1103/PhysRevLett.114.117201.

[8] J. Cao, S. Liang, C. Zhang, Y. Liu, J. Huang, Z. Jin, Z.-G. Chen, Z. Wang, Q. Wang, J. Zhao, S. Li, X. Dai, J. Zou, Z. Xia, L. Li, F. Xiu, Landau level splitting in Cd_3As_2 under high magnetic fields, Nat. Commun. 6 (2015) 7779, https://doi.org/10.1038/ncomms8779.

[9] Y. Zhao, H. Liu, C. Zhang, H. Wang, J. Wang, Z. Lin, Y. Xing, H. Lu, J. Liu, Y. Wang, S.M. Brombosz, Z. Xiao, S. Jia, X.C. Xie, J. Wang, Anisotropic Fermi Surface and Quantum Limit Transport in High Mobility Three-Dimensional Dirac Semimetal Cd_3As_2, Phys. Rev. X 5 (2015), 031037, https://doi.org/10.1103/PhysRevX.5.031037.

[10] H. Wang, H. Wang, H. Liu, H. Lu, W. Yang, S. Jia, X.-J. Liu, X.C. Xie, J. Wei, J. Wang, Observation of superconductivity induced by a point contact on 3D Dirac semimetal Cd_3As_2 crystals, Nature materials 15 (2016), https://doi.org/10.1038/nmat4456, 38.

[11] C.-Z. Li, L.-X. Wang, H. Liu, J. Wang, Z.-M. Liao, D.-P. Yu, Giant negative magnetoresistance induced by the chiral anomaly in individual Cd_3As_2 nanowires, Nat. Commun. 6 (2015) 10137, https://doi.org/10.1038/ncomms10137.

[12] H. Yi, Z. Wang, C. Chen, Y. Shi, Y. Feng, A. Liang, Z. Xie, S. He, J. He, Y. Peng, X. Liu, Y. Liu, L. Zhao, G. Liu, X. Dong, J. Zhang, M. Nakatake, M. Arita, K. Shimada, H. Namatame, M. Taniguchi, Z. Xu, C. Chen, X. Dai, Z. Fang, X.J. Zhou, Evidence of topological surface state in three-dimensional Dirac semimetal Cd_3As_2, Sci. Rep. 4 (2014) 6106, https://doi.org/10.1038/srep06106.

[13] M. Neupane, S.-Y. Xu, N. Alidoust, R. Sankar, I. Belopolski, D.S. Sanchez, G. Bian, C. Liu, T.-R. Chang, H.-T. Jeng, B.K. Wang, G. Chang, H. Lin, A. Bansil, F. Chou, M.Z. Hasan, Surface versus bulk Dirac state tuning in a three-dimensional topological Dirac semimetal, Phys. Rev. B - Condens. Matter Mater. Phys. 91 (2015), 241114, https://doi.org/10.1103/PhysRevB.91.241114.

[14] B. Zhao, P. Cheng, H. Pan, S. Zhang, B. Wang, G. Wang, F. Xiu, F. Song, Weak antilocalization in Cd_3As_2 thin films, Sci. Rep. 6 (2016) 22377, https://doi.org/10.1038/srep22377.

[15] G. Abrosimova, A. Aronin, Amorphous and nanocrystalline metallic alloys, Progr. Metall. Alloys 9 (2016), https://doi.org/10.5772/61725.

[16] C.F. Holder, R.E. Schaak, Tutorial on powder X-ray diffraction for characterizing nanoscale materials, Acs Nano 13 (2019) 7359–7365, https://doi.org/10.1021/acsnano.9b05157.

[17] A.V. Suslov, A.B. Davydov, L.N. Oveshnikov, L.A. Morgun, K.I. Kugel, V.S. Zakhvalinskii, E.A. Pilyuk, A.V. Kochura, A.P. Kuzmenko, V.M. Pudalov, B. A. Aronzon, Observation of subkelvin superconductivity in Cd_3As_2 thin films, Phys. Rev. B 99 (2019), 094512, https://doi.org/10.1103/PhysRevB.99.094512.

[18] D. Koumoulis, R.E. Taylor, J. McCormick, Y.N. Ertas, L. Pan, X. Che, K.L. Wang, L.-S. Bouchard, Effects of Cd vacancies and unconventional spin dynamics in the Dirac semimetal Cd_3As_2, J. Chem. Phys. 147 (2017), 084706, https://doi.org/10.1063/1.4999467.

[19] H.-Z. Lu, S.-Q. Shen, Weak antilocalization and localization in disordered and interacting Weyl semimetals, Phys. Rev. B 92 (2015), 035203, https://doi.org/10.1103/physrevb.92.035203.

[20] I. Garate, L. Glazman, Weak localization and antilocalization in topological insulator thin films with coherent bulk-surface coupling, Phys. Rev. B 86 (2012), 035422, https://doi.org/10.1103/physrevb.86.035422.

[21] H.-Z. Lu, J. Shi, S.-Q. Shen, Competition between Weak Localization and Antilocalization in Topological Surface States, Phys. Rev. Lett. 107 (2011), 076801, https://doi.org/10.1103/physrevlett.107.076801.

[22] S. Hikami, A.I. Larkin, Y. Nagaoka, Spin-orbit interaction and magnetoresistance in the two dimensional random system, Prog. Theor. Phys. 63 (1980) 707–710, https://doi.org/10.1143/ptp.63.707.

[23] B.L. Altshuler, A.G. Aronov, D.E. Khmelnitsky, Effects of electron-electron collisions with small energy transfers on quantum localisation, J. Phys. C: Solid State Phys. 15 (1982) 7367–7386, https://doi.org/10.1088/0022-3719/15/36/018.

[24] H. Steinberg, J.-B. Laloe, V. Fatemi, J.S. Moodera, P. Jarillo-Herrero, Electrically tunable surface-to-bulk coherent coupling in topological insulator thin films, Phys. Rev. B 84 (2011), 233101, https://doi.org/10.1103/physrevb.84.233101.